Chapter II. SHORT-LIVED CELL-CELL INTERACTIONS FOSTER TRANSPORT-LIMITED CELL AGGREGATION: BIPHASIC DEPENDENCE OF AGGREGATION DYNAMICS ON SUBSTRATUM ADHESIVITY

1. Abstract

Multicellular aggregation is fundamental to development and tissue repair.[1-3] The classical equilibrium model for multicellular aggregation is based on differential cell adhesivity to its neighbors versus the underlying substratum.[4-6] In many biological contexts, however, dynamics is critical. Here, we demonstrate that multicellular aggregation dynamics involves both local adhesive interactions and transport by cell migration. Quantitative measurements by time-lapse video microscopy reveal that the lifetime of cell-cell interactions is shorter than the mean time between cell-cell collisions, suggesting aggregation may be transport-limited. Consistent with this hypothesis, the transient aggregate size exhibits a biphasic dependence on substratum adhesivity, matching independent measurements of the trend in cell migration speed. These results demonstrate that cell aggregation adheres to a transport-reaction model ascribed widely to physicochemical systems.[7, 8] Our findings have implications for the role of cell motility during developmental aggregation processes and provide design principles for tuning aggregation dynamics in applications such as tissue engineering.

Manuscript submitted for publication (April 2010).

2. Main Text

Multicellular aggregation is fundamental to embryonic development and tissue repair,[1-3] and the loss of aggregate integrity is associated with pathologies such as metastasis.[9] The classical paradigm is that the equilibrium state of aggregation is determined by minimizing the adhesive free energy of the system.[4-6] This model predicts that if the cumulative strength of cell-cell adhesion (as quantified by the number and affinity of receptor-ligand bonds) exceeds the strength of cell-substratum adhesion, cells will organize into aggregates. Conversely, if the strength of cell-substratum adhesion exceeds the strength of cell-cell adhesion, cells will adopt a dispersed phenotype. This monotonic relationship between aggregation and substratum adhesivity has been demonstrated experimentally.[10] When cells of equal cohesivity are employed, those seeded onto weakly adhesive substrata aggregate while those seeded onto highly adhesive substrata dissociate.

In many biological contexts, however, the dynamics of aggregation is likely to be critical. The development of tissues and organs proceeds through multiple stages, and each step, such as multicellular aggregation, must be accomplished within a defined time window. When considering dynamics, it is well-established in physicochemical systems ranging from colloids[7] to atmospheric chemistry[8] that aggregation must be viewed as a two-step process (Figure II-1). The individual particles must first "find" each other (a transport step) and then form stable contacts (a reaction step). Aggregation dynamics is dictated by the slower of the two steps. It remains to be elucidated, however, whether cellular aggregation dynamics follows a similar principle.

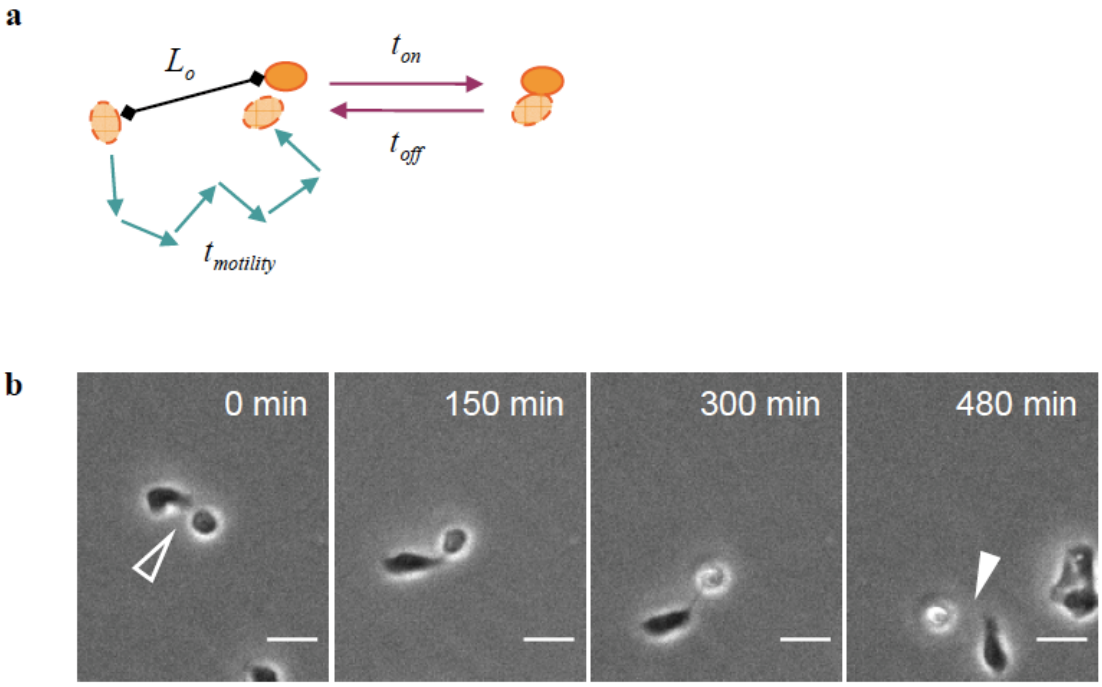

Figure II-1. Two-step model for multicellular aggregation dynamics.

(a) To form aggregates, distant cells must first move close together (a transport step) and then undertake reversible cell-cell interactions (a reaction step). Transport occurs by cell migration, and the mean time to collide ($t_{motility}$) depends on the mean initial spacing between cells (L_o) and the speed and persistence of cell movement. Meanwhile, the local cell-cell interaction involves adhesion (t_{on}) and detachment (t_{off}). (b) Timelapse images of migrating MDCK cells show the initiation of cell-cell contact (open arrowhead) and the subsequent detachment (closed arrowhead). Because t_{on} and t_{off} cannot be distinguished experimentally, timelapse images were used to quantify the total duration of cell-cell interactions ($t_{adhesion}$) as a lumped measure of t_{on} and t_{off}. Scale bar, 25 μm.

It is currently difficult to evaluate whether transport by cell migration or local cell-cell "reactivity" is the rate-limiting step in multicellular aggregation. In contrast to the large body of quantitative studies of cell migration[11], to our knowledge, there is currently no evaluation of the timescale on which migrating cells "react" to form intercellular contacts. Although cell-cell contact dynamics has been studied for cells brought together with micropipettes[12], interactions between migrating cells are likely to

be significantly different. Migrating cells interact with each other while concomitantly adhering to an underlying substratum. Furthermore, these cell-cell and cell-substratum adhesions involve common molecular components and physical machinery, such as actin and cell-generated contractile forces, respectively.[13, 14]

To quantify the dynamics of cell-cell interactions, we identified cell-cell collisions in time-lapse videos and recorded the duration of intercellular contact. These measurements were performed using substrata coated with different amounts of the adhesion ligand laminin (Ln) in order to better understand how varying substratum adhesivity affects the lifetime of cell-cell interactions. We observe that the mean lifetime of cell-cell interactions ($t_{adhesion}$) exhibits a monotonic dependence on substratum adhesivity (Figure II-2). Increasing adhesion ligand density reduces the lifetime of cell-cell interactions: $t_{adhesion}$ is nearly 600 min on substrata of low adhesivity and is reduced to approximately 200 min on substrata of high adhesivity. To confirm that our measurements are capturing specific cell-cell interactions, we treated cells with an antibody (DECMA) that blocks E-cadherin, a cell surface receptor that mediates intercellular adhesion. Treatment with DECMA reduces $t_{adhesion}$ compared to treatment with a non-specific IgG control, confirming that E-cadherin is involved in mediating these cell-cell interactions (Figure II-4, Supplemental Data).

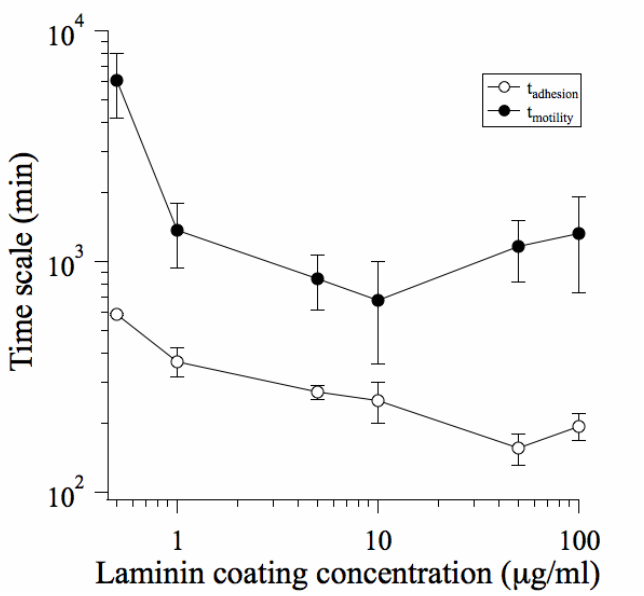

Figure II-2. The dependence of timescales of local cell-cell reactivity (tadhesion) and transport (tmotility) on substratum adhesivity.

The duration of cell-cell interactions ($t_{adhesion}$) and the mean time for nearest neighbors to collide ($t_{motility}$) were quantified for substrata prepared with different coating concentrations of Ln. Error bars, SEM (n = 2-3).

To assess how the measured lifetime of cell-cell interactions compares with the timescale of transport, we next examined cell migration on Ln-coated substrata. Cell migration in an isotropic environment exhibits an unbiased persistent random walk characterized by a diffusivity or motility coefficient (μ) that is related to the speed (S) and directional persistence (P) of cell movement.[15, 16] Migrating cells were tracked using time-lapse video microscopy, and cell speed was determined by fitting mean squared displacements to a persistent random walk model. Cell speed exhibits the expected biphasic dependence on substratum adhesivity.[11] In our system, the peak cell speed was 0.77 ± 0.09 μm/min on substrata coated with 10 μg/mL Ln (Figure II-5, Supplemental Data). The measured values of S and P (29.1 ± 6.4 min) are consistent with published values for epithelial cell lines.[17-19]

Using these values for S and P, we calculated the mean time required for a cell to collide with its nearest neighbor ($t_{motility} = L_o^2/\mu$) where $L_o \sim 108$ μm is the mean intercellular spacing based on the initial cell density of 8.5×10^3 cells/cm^2 and the motility coefficient μ is equal to S^2P. This time scale for transport exhibits a biphasic dependence on substratum adhesivity; therefore cell-cell collisions are infrequent on substrata of low and high adhesivity ($t_{motility} = 6.1 \pm 1.8 \times 10^3$ and $1.3 \pm 0.6 \times 10^3$ min, respectively) and occur with greatest frequency on substrata of moderate adhesivity ($t_{motility} = 6.8 \pm 3.2 \times 10^2$ min) (Figure II-2).

Comparing the measured time scales of transport and local reactivity reveals that $t_{motility}$ is greater than $t_{adhesion}$ across the complete range of Ln coating concentrations. Therefore, if multicellular systems follow the general two-step principle of aggregation dynamics, we would expect aggregation dynamics to exhibit a biphasic dependence on substratum adhesivity. Testing this hypothesis, however, is not straightforward. Varying substratum adhesivity will affect the number of seeded cells that attach to the substratum, thereby introducing unwanted differences in initial intercellular spacing. In addition, adequate time must be allowed for cells to attach to the substratum – a particularly important concern for substrata of low adhesivity. Furthermore, any non-adherent cells must be removed to ensure that the observed multicellular aggregation is the result of collisions between adherent, migrating cells and not between drifting cells in suspension. Guided by these and other considerations, we developed a rigorous protocol for studying the effect of substratum adhesivity on multicellular aggregation dynamics (Supplemental

Methods). Our method yields highly uniform initial conditions: for all Ln coating concentrations, the initial density of substratum-attached cells was $8.5 \pm 0.2 \times 10^3$ #/cm^2 (Table II-1, Supplemental Data).

To quantify aggregate sizes, two-channel fluorescence images were acquired of multicellular aggregates stained with a nuclear and cell membrane marker. The mean number of cells per aggregate was determined using previously described automated image processing techniques.[20] We first performed a time course study to identify an appropriate time-point at which to examine the dynamics of our system. Mean aggregate size was found to increase monotonically with time until reaching a plateau after 20 h of incubation (Figure II-6, Supplemental Data). Therefore, we selected 15 h as an appropriate incubation time for capturing aggregation dynamics.

The mean aggregate size at 15 h exhibits a biphasic dependence on substratum adhesivity (Figure II-3). Moreover, the maximum aggregate size occurs at the Ln coating concentration of 10 μg/ml, matching the conditions at which cell speed is maximum. These findings are consistent with a two-step physiochemical model for multicellular aggregation dynamics. Furthermore, these data demonstrate that the time scale of local reactivity is sufficiently fast (200-600 min) to render aggregation dynamics transport-limited. The consequence is that aggregation dynamics follows a non-monotonic dependence on substratum adhesivity, qualitatively contrary to the equilibrium perspective of the differential adhesion paradigm.

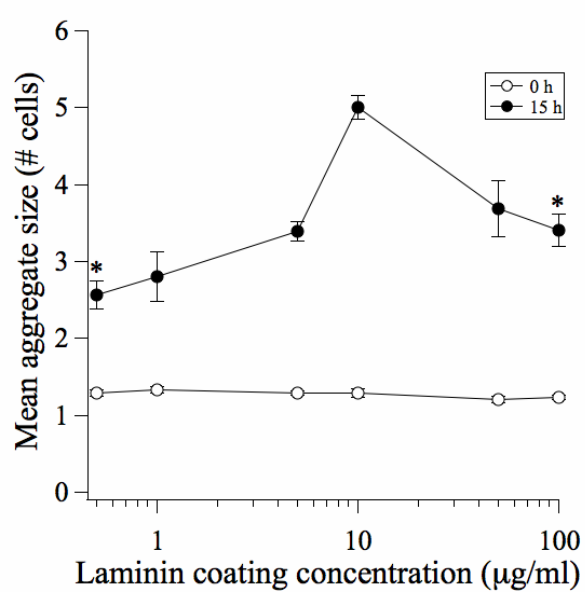

Figure II-3. Biphasic dependence of aggregate size on substratum adhesivity: evidence for motility-limited aggregation dynamics.

The mean aggregate size (# cells per aggregate) was quantified at initial time (0 h) and 15 h after the attachment of MDCK cells to Ln-coated substrata. Error bars, SEM (n = 3-4). *, $p < 0.05$ in comparing to the 10 μg/mL condition.

Our findings establish a key role for cell motility in multicellular aggregation. Evidence is also mounting for the role of cell motility in mediating another multicellular process: cell sorting of heterogeneous cell populations. Though proposed years ago as a potential mediator of cell sorting, differential motility has only recently been discussed as a driving mechanism for this phenomenon.[21, 22] A recent mathematical model of *Dictyostelium* slug formation, for example, demonstrates that motility differences among cell types are sufficient to create the defined spatial pattern of cells observed in migrating slugs.[23] In addition, cellular rearrangements within epithelial tissues have been attributed to differential motility: cells expressing high levels of the enzyme MMP14, which preferentially localize to the tip of epithelial tubes, were found to be faster and more directionally persistent than their low-expressing counterparts.[19] These studies of cell

sorting together with our results pertaining to cellular aggregation demonstrate the emerging importance of cell motility in the dynamics of multicellular re-arrangements.

In addition to natural developmental processes, our findings have direct implications for tissue engineering. Although engineering biomaterials with reduced adhesivity may enhance aggregation at equilibrium[24], we demonstrate that a qualitatively distinct strategy is needed to ensure optimal kinetics of aggregation. When dynamics is the chief concern, we propose that the design strategy must account for whether transport or local cell-cell reactivity is rate-limiting. Where transport is rate-limiting, a biomaterial with intermediate adhesivity will provide maximal aggregation dynamics. In conclusion, our results provide a dynamical physical perspective on engineering microenvironments to promote multicellular aggregation, an important precursor to more mature multicellular structures and tissues.

3. Acknowledgements

We thank members of the Asthagiri laboratory for helpful discussions. This work was supported by the National Institutes of Health grant R01-CA138899 and the Jacobs Institute for Molecular Engineering for Medicine. M.D. Pope was supported by a National Science Foundation Graduate Research Fellowship and an NIH Molecular Cell Biology Training Grant (NIH/NRSA5T32GM07616Z).

4. Materials and Methods

4.1. Substratum preparation

Tissue culture-treated polystyrene dishes (Corning) were incubated overnight at 4°C with laminin (Sigma) diluted in PBS. Prior to use, dishes were blocked with 1 mg/mL heat-inactivated (55 C for 1 hour) BSA (Sigma) in PBS at 37^{o}C for 1 h.

4.2. Cell culture

MDCK cells were cultured in Dulbecco's modified Eagle's medium (DMEM, Invitrogen) supplemented with 10% (v/v) fetal bovine serum (Invitrogen) and 1% (v/v) penicillin/streptomycin (Invitrogen). For collision, motility and aggregation assays, confluent MDCK monolayers were suspended by treatment with 0.25% trypsin/53 mM EDTA (Invitrogen) for 5 minutes at 37 C and plated at the desired cell density in serum-free medium (SFM: DMEM supplemented with 1% (v/v) penicillin/streptomycin and 1 mg/mL BSA (Sigma)) supplemented with 20 ng/mL epidermal growth factor (EGF) (Peprotech). After allowing cells to adhere to the substratum for 1 – 3 hours, non-adherent cells were washed and the remaining adherent cells were incubated in fresh SFM supplemented with 20 ng/mL EGF.

4.3. Quantification of cell-cell adhesion dynamics

Samples were imaged via time-lapse microscopy using a Zeiss Axiovert 200M microscope equipped with a digital CCD camera and an environmental chamber that

maintains temperature, humidity and CO_2 levels. 5x phase contrast images were collected every 5 minutes for 24 hours. Cell-cell interactions that were initiated in the first 12 hours of observation were tracked, and the duration of cell-cell contact was recorded. Interacting cell pairs observed to collide with an additional cell or group of cells were excluded from the analysis.

4.4. Quantification of migration speeds

Migration tracks of individual cells were imaged by time-lapse microscopy. 10x phase contrast images were collected every 15 minutes for 15 hours. Nuclei of isolated cells were marked using ImageJ software (National Institutes of Health), and mean squared displacements were determined for each cell using overlapping intervals.[16] The mean squared displacements were averaged and fit to a persistent random walk model to calculate cell speed, S, and persistence time, P: $\langle d^2(t) \rangle = 2S^2P[t-P(1-e^{-t/P})]$.[15, 16] Persistence was averaged across all laminin coating concentrations to determine a mean persistence time.

4.5. Quantification of aggregate size

Samples were fixed in formalin (Sigma), incubated overnight at 4 C in PBS + 100 mM glycine (Sigma), then permeabilized in PBS + 0.2% Triton-X for 10 minutes at 4 C. Cells were stained with DAPI and the membrane dye FM-464FX (Molecular Probes). Fluorescence images were captured at 10x magnification using a Zeiss Axiovert 200M microscope equipped with a digital CCD camera. 49 non-overlapping fields were imaged

per sample. Aggregate sizes were determined from these images using thresholding and edge detection algorithms as previously described.[20] The number of nuclei per field was also quantified in order to calculate the density of substratum-attached cells.

5. Supplemental Methods

In order to study how local cell-cell reactivity and transport by cell migration affect aggregation dynamics, it is essential to ensure that (1) isolated cells (not pre-formed aggregates) are seeded initially on the substrata, (2) any non-adherent cells are removed to prevent them from drifting and binding to adherent cells/aggregates, and (3) the initial density of isolated cells (and, therefore the initial mean intercellular spacing) is equal among all samples.

To address these considerations, MDCK cells were suspended using traditional cell dissociation techniques, and a desired concentration of single cells (N_c) was seeded onto Ln-coated substrata. After incubating cells for an appropriate duration (t_{inc}) to allow cell adhesion onto the substratum, non-adherent cells were removed by medium aspiration. The key issue, however, lies in determining the appropriate values for N_c and t_{inc} to ensure that the initial cell density on the substratum is equal for all Ln coating concentrations.

We reasoned that cell adhesion to a substratum is likely to proceed more quickly on substrata coated with higher Ln density than on those coated with low amounts of Ln based on reported measurements of cell spreading kinetics on protein-coated surfaces.[25] We quantified the dynamics of cell adhesion in our system (MDCK cells adhering to Ln-coated tissue culture plastic) (Figure II-7, Supplemental Data) and chose an incubation time that allows cell adhesion to reach its maximum saturation value for each Ln coating

concentration (Table II-2, Supplemental Data). This incubation time varied between 1-3 h and is much shorter than the time at which aggregation is quantified (15 h after t_{inc}).

In addition to the time of incubation, careful attention was given to the concentration of cells (N_c) seeded for each Ln coating concentration. We observed that the fraction of seeded cells that attach to the substratum at t_{inc} varied with Ln coating concentration (Figure II-8, Supplemental Data). Therefore, to ensure equivalent initial cell density among the different Ln-coated substrata, we seeded a greater concentration of cells (N_c) on substrata coated with lower amounts of Ln than on those coated with higher Ln density. Because the fraction of adherent cells was likely to also vary between trials, we took an additional precaution by performing each trial as follows: duplicate sets of cell suspensions containing three closely-spaced N_c were seeded for each Ln coating concentration (Table II-3, Supplemental Data). The first set of triplicates was used to determine the seeding concentration that yielded an initial cell density of approximately 8.5×10^3 #/cm^2. Once identified, the corresponding sample in the second set was used to determine aggregate size at 15 h. In this manner, we ensured that aggregation dynamics were quantified among samples that had an equivalent initial cell density (Table II-1, Supplemental Data).

6. Supplemental Data

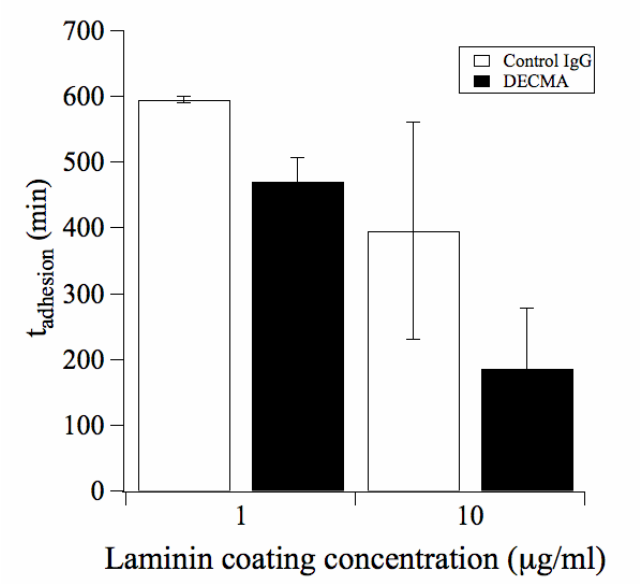

Figure II-4. Effect of antibody treatments on the lifetime of cell-cell interactions.

The lifetime of cell-cell adhesions ($t_{adhesion}$) was measured in the presence of an E-cadherin-specific or non-specific control IgG. Error bars, SEM (n = 2).

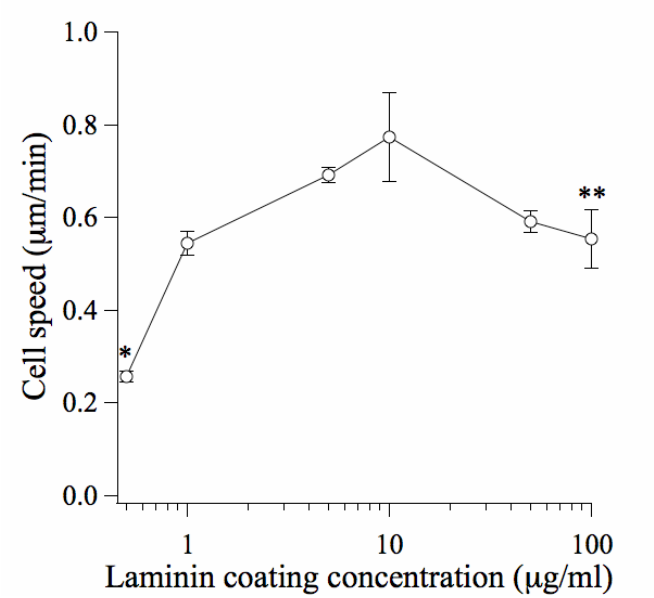

Figure II-5. Cell speed exhibits a biphasic dependence on surface adhesivity.

The migration tracks of individual MDCK cells were traced using timelapse microscopy. Mean squared displacements were calculated and fit to a persistent random walk model to determine cell speed.[15, 16] Error bars, SEM (n = 2). *, $p<0.05$ and **, $p<0.1$ in comparing to the 10 μg/mL condition.

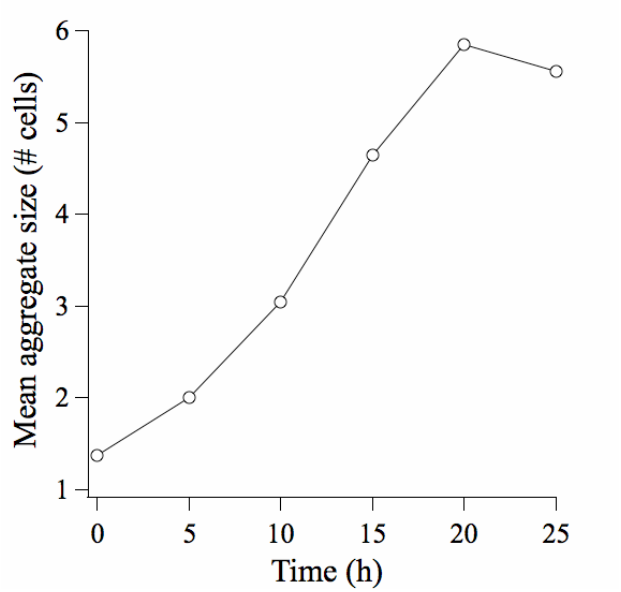

Figure II-6. Time-course of aggregate assembly.

The mean aggregate size (# of cells per aggregate) was quantified at initial time (0 h) and at multiple timepoints after the attachment of MDCK cells to the Ln-coated (10 μg/mL) substratum (n = 1).

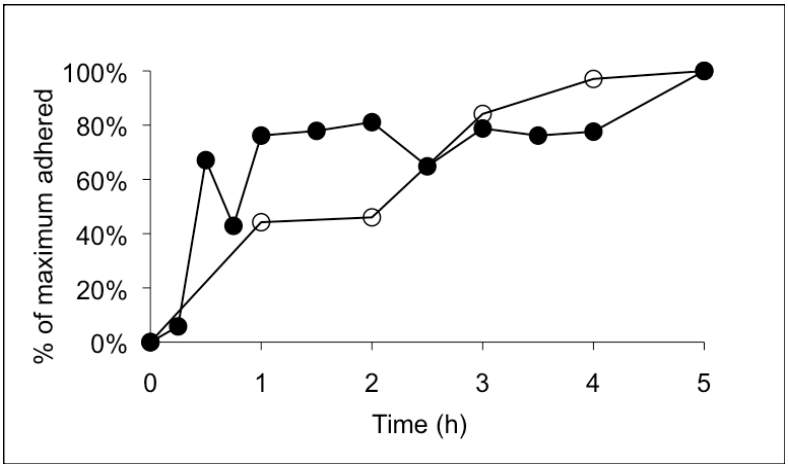

Figure II-7. Substratum adhesivity affects the rate of cell attachment to the substratum.

1.5×10^5 MDCK cells were seeded onto substrata coated with 0.5 μg/mL or 5 μg/mL Ln. After incubation for the indicated times, the non-adherent cells were washed, and the number of cells that remain attached was determined. The percent cells adhered relative to the maximum saturation value is shown (n = 1).

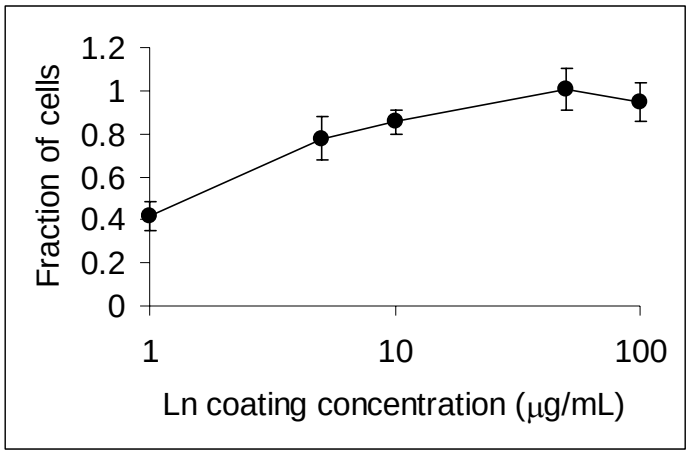

Figure II-8. Substratum adhesivity affects the fraction of seeded cells that attach.

1.0 x 10^5 MDCK cells were seeded onto Ln-coated substrata. The fraction of cells that attached to each substratum was quantified after incubation for t_{inc} (1 – 3 h) (n = 3-4).

Table II-1. Initial density of substratum-attached cells.

The number of substratum-attached cells per unit surface area was quantified at initial time (0 h) from fluorescence images of MDCK cells stained with DAPI. Error bars, SEM (n = 3-4).

Ln coating concentration (μg/mL)	0.5	1	5	10	50	100
Initial cell surface density x 10^{-3} (#/cm^2)	8.3 ± 0.78	8.2 ± 0.32	9.1 ± 0.50	8.9 ± 0.59	8.2 ± 0.59	8.2 ± 0.20

Table II-2. Incubation times for Ln-coated substrata.

Ln coating concentration (μg/mL)	0.5	1	5	10	50	100
t_{inc} (h)	3		2		1	

Table II-3. Cell seeding concentrations for Ln-coated substrata.

	N_c x 10^{-4} (#/mL)					
Ln coating concentration (μg/mL)	3.75	5.0	6.75	7.5	10.0	12.5
0.5				X	X	X
1			X	X	X	
5		X	X	X		
10		X	X	X		
50	X	X	X			
100	X	X	X			

7. References

1. Gumbiner BM. Cell adhesion: the molecular basis of tissue architecture and morphogenesis. Cell 1996; 84:345-57.
2. Nakagawa S, Takeichi M. Neural crest cell-cell adhesion controlled by sequential and subpopulation-specific expression of novel cadherins. Development (Cambridge, England) 1995; 121:1321-32.
3. Oberlender SA, Tuan RS. Expression and functional involvement of N-cadherin in embryonic limb chondrogenesis. Development (Cambridge, England) 1994; 120:177-87.
4. Steinberg MS. On Mechanism of Tissue Reconstruction by Dissociated Cells .3. Free Energy Relations and Reorganization of Fused, Heteronomic Tissue Fragments. Proceedings of the National Academy of Sciences of the United States of America 1962; 48:1769-&.
5. Steinberg MS. Differential adhesion in morphogenesis: a modern view. Current opinion in genetics & development 2007; 17:281-6.
6. Steinberg MS, Foty RA. Intercellular adhesions as determinants of tissue assembly and malignant invasion. Journal of cellular physiology 1997; 173:135-9.
7. Lin MY, Lindsay HM, Weitz DA, Ball RC, Klein R, Meakin P. Universality in Colloid Aggregation. Nature 1989; 339:360-2.
8. Seinfeld J, Pandis S. *Atmospheric Chemistry and Physics: From Air Pollution to Climate Change* (Wiley, Hoboken, 2006).
9. Hanahan D, Weinberg RA. The hallmarks of cancer. Cell 2000; 100:57-70.

10. Ryan PL, Foty RA, Kohn J, Steinberg MS. Tissue spreading on implantable substrates is a competitive outcome of cell-cell vs. cell-substratum adhesivity. Proceedings of the National Academy of Sciences of the United States of America 2001; 98:4323-7.

11. Palecek SP, Loftus JC, Ginsberg MH, Lauffenburger DA, Horwitz AF. Integrin-ligand binding properties govern cell migration speed through cell-substratum adhesiveness. Nature 1997; 385:537-40.

12. Sung KL, Sung LA, Crimmins M, Burakoff SJ, Chien S. Determination of junction avidity of cytolytic T cell and target cell. Science 1986; 234:1405-8.

13. Hartsock A, Nelson WJ. Adherens and tight junctions: structure, function and connections to the actin cytoskeleton. Biochimica et biophysica acta 2008; 1778:660-9.

14. Ridley AJ, Schwartz MA, Burridge K, Firtel RA, Ginsberg MH, Borisy G, Parsons JT, Horwitz AR. Cell migration: integrating signals from front to back. Science 2003; 302:1704-9.

15. Dickinson RB, Tranquillo RT. Optimal Estimation of Cell-Movement Indexes from the Statistical-Analysis of Cell Tracking Data. Aiche J 1993; 39:1995-2010.

16. Walmod PS, Hartmann-Petersen R, Berezin A, Prag S, Kiselyov VV, Berezin V, Bock E. Evaluation of individual-cell motility. Methods in molecular biology (Clifton, NJ 2001; 161:59-83.

17. Li Y, Bhargava MM, Joseph A, Jin L, Rosen EM, Goldberg ID. Effect of hepatocyte growth factor/scatter factor and other growth factors on motility and

morphology of non-tumorigenic and tumor cells. In vitro cellular & developmental biology 1994; 30A:105-10.

18. Maheshwari G, Wiley HS, Lauffenburger DA. Autocrine epidermal growth factor signaling stimulates directionally persistent mammary epithelial cell migration. The Journal of cell biology 2001; 155:1123-8.

19. Mori H, Gjorevski N, Inman JL, Bissell MJ, Nelson CM. Self-organization of engineered epithelial tubules by differential cellular motility. Proceedings of the National Academy of Sciences of the United States of America 2009; 106:14890-5.

20. Pope MD, Graham NA, Huang BK, Asthagiri AR. Automated quantitative analysis of epithelial cell scatter. Cell adhesion & migration 2008; 2:110-6.

21. Stefanelli A ZA CV. Retinal reconstitution in vitro after disaggregation of embryonic chicken eyes. Acta Embryol Morphol Exper 1961; 4:47-55.

22. Townes PL, Holtfreter J. Directed Movements and Selective Adhesion of Embryonic Amphibian Cells. J Exp Zool 1955; 128:53-120.

23. Umeda T, Inouye K. Cell sorting by differential cell motility: a model for pattern formation in Dictyostelium. Journal of theoretical biology 2004; 226:215-24.

24. Powers MJ, Rodriguez RE, Griffith LG. Cell-substratum adhesion strength as a determinant of hepatocyte aggregate morphology. Biotechnology and bioengineering 1997; 53:415-26.

25. Dubin-Thaler BJ, Giannone G, Dobereiner HG, Sheetz MP. Nanometer analysis of cell spreading on matrix-coated surfaces reveals two distinct cell states and STEPs. Biophysical journal 2004; 86:1794-806.